

RSC Advances



This is an *Accepted Manuscript*, which has been through the Royal Society of Chemistry peer review process and has been accepted for publication.

Accepted Manuscripts are published online shortly after acceptance, before technical editing, formatting and proof reading. Using this free service, authors can make their results available to the community, in citable form, before we publish the edited article. This *Accepted Manuscript* will be replaced by the edited, formatted and paginated article as soon as this is available.

You can find more information about *Accepted Manuscripts* in the [Information for Authors](#).

Please note that technical editing may introduce minor changes to the text and/or graphics, which may alter content. The journal's standard [Terms & Conditions](#) and the [Ethical guidelines](#) still apply. In no event shall the Royal Society of Chemistry be held responsible for any errors or omissions in this *Accepted Manuscript* or any consequences arising from the use of any information it contains.

ARTICLE

Highly monodispersed Ag embedded SiO₂ nanostructured thin film for Sensitive SERS substrate: Growth, characterization and Detection of dye molecules

Naidu Dhanpal Jayram^a, S. Sonia^a, P. Suresh Kumar^b, L. Marimuthu^a, Yoshitake Masuda^c, D. Mangalaraj^{a*}, N. Ponpandian^a, C. Viswanathan^a, Seeram Ramakrishna^d

Cite this: DOI:
10.1039/x0xx00000x

Received 00th January 2015,
Accepted 00th January 2015

DOI: 10.1039/x0xx00000x

www.rsc.org/

Highly monodispersed Ag embedded SiO₂ nanostructured thin films have been synthesized and their sensitivity towards SERS investigated. The possible mechanism for the formation of a highly monodispersed SiO₂ nanostructured thin film and its self-assembled nanogap with Ag are discussed. It is found that the architecture of Ag embedded SiO₂ (Ag@SiO₂) is drastically influenced by the concentration of the precursors and the reaction time. Morphology and monodispersity of the silica thin film were confirmed using FESEM and AFM. Crystallinity and existence of Ag on SiO₂ were confirmed using XRD and XPS. The substrate shows enhanced SERS efficiency due to the reduced size (around 15 nm) of the Ag nanoparticles and the nano gap of (below 3 nm) between SiO₂ and Ag. Based on the FDTD (finite-difference time-domain) simulation, the creation of hotspots was confirmed for the obtained nanogap. The prepared thin film possesses strong Surface Plasmon Resonance (SPR) with widely tunable peaks between 407–430 nm in the UV visible spectrum. The Ag@SiO₂ nanospheres-based SERS platform provides highly enhanced effects and reveals a reproducible enhancement ($EF = 7.79 \times 10^8$) of R6G (Rhodamine 6G), allowing a detection limit from a 10^{-18} mol L⁻¹ solution. The prepared substrate was also used to detect trace level of melamine from a 10^{-8} mol L⁻¹ solution.

1. Introduction

Plasmonics substrates offer a unique opportunity for manipulating the interaction between light and matter at the nanoscale. The assembly of plasmonic nanoparticles onto planar ensembles with short interparticle distances leads to novel and unique optoelectronic features due to long-range plasmon coupling over large areas.¹ These extended plasmonic structures proposed as advanced platforms to address biological and medical challenges. In recent years, Surface Enhanced Raman Spectroscopy (SERS) analysis has developed into a noteworthy tool in various fields such as analytical chemistry, environmental monitoring, forensics and biology due to its Localized Surface Plasmon Resonance (LSPR) in nanostructured metal surfaces.^{2–3} Surface enhanced Raman Scattering (SERS) mediated by plasmonic nanostructured substrates is rapidly being established as a reliable detection and analysis spectroscopic technique in the biological and medical fields.¹ Therefore, suitable substrates for SERS analysis of biological samples are most desirable. The most critical aspect of SERS measurement is the nanostructure used to enhance the Raman signal.^{4–5} However metal oxides are also preferred in view of their semiconducting properties, shape and size as well as their local dielectric environment for light scattering and coupling efficiency.⁶ The construction of novel metal nanostructured thin films has therefore developed into an increasingly important research area in the fabrication of SERS substrates.^{7–9} Noble metal nanostructures are commonly used for SERS studies due to their

strong dependence on morphology and Localized Surface Plasmon Resonance. The functional properties of nanostructured films are largely determined by the size, morphology, surface properties and composition of the nanoparticles within the film. For practical use, such nanostructured films should have uniformity,¹⁰ roughness,¹¹ and growth orientation.^{12–13} Apart from this, the gap between two nanoparticles in nanostructured films should lead to enhanced Raman amplification by creating hot spots.¹⁴ However to create such hot spots at nanoscale junctions or interstices in a facile way is the major challenge in SERS among the researchers. For fabrication of such substrates one has to control reaction parameters such as solvent, temperature, and time which will influence the particle morphology during the growth process and such delicate manipulations can be used to obtain the controlled nanostructured films. In the present study, we are able to create such nanogaps using a facile vertical deposition technique. The isotropic growth of the synthesized nanospheres agrees with the physical and chemical concepts used to control the shape of nanostructures during the growth process, and also with the electro kinetic potential in colloidal solution; insight is gained into the mechanisms of both. Thus all parameters influence the resulting particle morphology during the vertical deposition process. In respect to this the metal film over nanospheres (FON) has shown effective SERS for structures having appropriate gap and diameter ratio. A Variety of metal oxides like SiO₂, Fe₂O₃, CuO, ZnO, and TiO₂ have been used

as a SERS substrates.¹⁵⁻¹⁶ Among them SiO_2 serves as a striking supportive material and stable coating to stabilize the metallic phase and to disperse the noble metal for the formation of reliable nanostructures.¹⁷⁻¹⁸ Ag embedded fumed silica based substrate offers the advantage of high roughness and prevents aggregation of Ag nanoparticles, thus stabilizing the SERS effect, leading to self-assembled nanospheres. There are many reports on $\text{Ag}@\text{SiO}_2$ nanocomposites for ultrasensitive detection with highly enhanced effects. Also prodigious methods have been used to synthesize nanospheres by chemical methods and physical techniques such as vacuum coating, sputtering and plasma etching.¹⁹⁻²¹ In all the above techniques silica plays the major role of the base layer due to its monodispersity and also acts like a template for silver deposition. Even though these techniques show highly enhanced SERS effects, only a few reports²²⁻²⁵ are available about the hot spots of SERS and self-assembled nanogaps. Recently Jing Chen et. al.²⁶ have reported similar results. They showed that broccoli-shaped Ag deposited on SiO_2 colloidal crystal templates by physical deposition technique gives good enhancement. The present work shows the formation of nano gap and self-assembling of silver NPs between silica by simple dip coating technique for the first time. Even though the chemical deposition technique has its own drawbacks, the highest enhancement is observed in this technique as reported by Yhang et. al.²⁵ A Similar work by Shijia Long et. al.¹⁸ also shows that R6G adsorbed on the substrate exhibits strong Raman signals, resulting from surface plasma coupling between closely spaced Ag nanoparticles. The present work, for the first time, demonstrates the creation of nanogap and high enhancement factor for detection of R6G dye on highly mono dispersed Ag embedded SiO_2 nanostructured thin film. The study of adherence of silver nanoparticles and self-assembled nanogaps between silver and silica nanospheres gives a clear idea of hotspots in silver embedded silica nanospheres and the creation of these hotspots was confirmed by FDTD simulation. The growth mechanism of self-assembled nanospheres and nanogaps for fabrication of SERS substrate is discussed via morphological imagery. The role of positive and negative charges of silver nanoparticles on silica nanospheres for SERS analysis has also been investigated.

2. Experimental

2.2 Synthesis of $\text{Ag}@\text{SiO}_2$

$\text{Ag}@\text{SiO}_2$ monodispersed nanospheres were synthesized by base-catalyzed hydrolysis of TEOS (Tetraethyl orthosilicate) using Stober method. Prior to SERS substrate preparation, glass substrates were cut to dimensions of $1 \times 2 \text{ cm}^2$ and carefully treated by the standard cleaning process which has been described in our previous publication.²⁷ The cleaned substrates were then dipped into the silica solution for two hours and dried at room temperature to obtain silica nanospheres. The dried substrates were immersed into Ag sol to synthesize $\text{Ag}@\text{SiO}_2$ nanospheres. Ag sol was prepared as follows: 10 ml of 0.02 M AgNO_3 was added drop by drop into a mixture of 10 ml of 0.375 M PVP and 10 ml of 0.1 M tri-sodium citrate with vigorous stirring at 80°C until a yellow color solution (Ag hydrosol A) was obtained. The above procedure was repeated using NaBH_4 as the reducing agent instead of trisodium citrate for the synthesis of Ag hydrosol B (Red colour). The schematic illustration is shown in

Fig.1 for the formation of $\text{Ag}@\text{SiO}_2$ thin film. The obtained film was further used as SERS substrate for detection of R6G and melamine. The probe molecule has been put onto film using micropipette and dried naturally.

2.2 Characterization technique

The prepared $\text{Ag}@\text{SiO}_2$ nanostructured thin films were used as SERS substrates and characterized using X-ray diffraction (XRD) pattern obtained using a Panalytical X'Pert Pro with $\text{Cu-K}\alpha$ radiation (1.5406 \AA), X-ray photoelectron spectroscopy (Kratos analytical, ESCA-3400, Shimadzu), UV- Vis spectrometer (Jasco V-640), FE-SEM (quanta-250), HR-TEM using JEOL JEM 2100, Atomic force microscopy (Veeco di - caliber) and Zeta size analyzer (Zeta sizer-s). SERS spectra were recorded using Raman spectrometer (LABRAM-HR) with laser excitation lines of 514 nm at room temperature.

3. Results and Discussion

3.1. Characterization of self-assembled $\text{Ag}@\text{SiO}_2$ thin films

Fig.2 shows the XRD pattern of the $\text{Ag}@\text{SiO}_2$ nanospheres. All the diffraction peaks are found to be well matched with the standard JCPDS (PDF# 893722) data. No characteristic impurity peaks like Ag_2O or AgO were detected. The strong and sharp diffraction peak observed at 38.627° for the corresponding plane (111) shows the face centered cubic structure of Ag nanoparticles and their crystalline nature. Due to its amorphous nature (See Fig. S1 \dagger), no diffraction peaks corresponding to SiO_2 were observed.

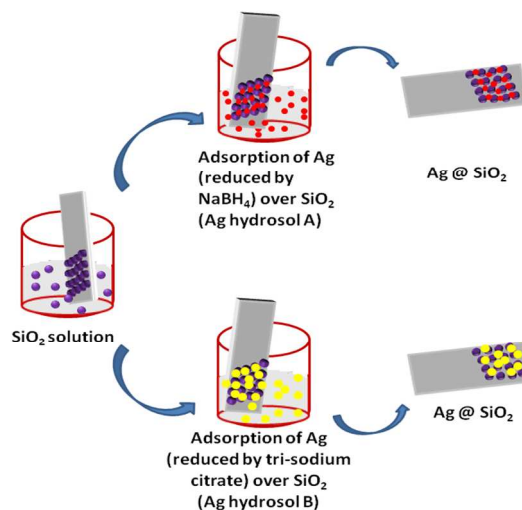


Fig.1. Schematic illustration of formation of Ag embedded silica ($\text{Ag}@\text{SiO}_2$) nanospheres

From the SAED pattern of TEM analysis we confirmed that the prepared nanoparticles are polycrystalline. The calculated lattice constant values $a = b = c = 4.0344 \text{ \AA}$ are consistent with the standard JCPDS data. Fig. 3(a-b) shows the XPS spectrum of Ag embedded silica which confirms the presence of metallic silver. The Ag 3d core level signals can be well fitted with the two peaks at binding energy values of 373.7 eV and 367.7 eV, corresponding to the $\text{Ag-3d}_{3/2}$ and $\text{Ag-3d}_{5/2}$ signals respectively. The XPS data substantiate that Ag nanospheres are self-assembled on the Si surface by Ag-Si chemical bonds.²⁸ Also, the doublet peaks located at 367.7 and 373.7 eV can

be assigned to Ag (0) according to a previous report.²⁹ These results indicate that the oxidation state of Si in the Ag@SiO₂ nanospheres is well sustained during the vertical growth deposition. So the LSPR that occurred between them could be confirmed for SERS intensity.

The prepared Ag and Ag@SiO₂ nanostructured thin films were dispersed in ethanol and subjected to UV-Visible spectroscopy analysis. The reduction of Ag (I) to zero valent Ag nanoparticles was confirmed by the colour change of solution from colorless to yellow (Ag hydrosol A) and colorless to red (Ag hydrosol B)³⁰ which correspond to absorption peaks at 429.24 and 407.28 nm respectively which are shown in Fig.4. Ag nanoparticles exhibit surface plasmon resonances which are mostly sharp and well separated from interband transitions.

The red shift of the absorption wavelength and the broadening of the band for Ag hydrosol A are related to the larger particles. This is due to the dipole-dipole interaction among Ag nanoparticles deposited on the dielectric silica nanosphere and also electromagnetic coupling which enhances the polarizability of the electron cloud resulting in red shift of Surface Plasmon Resonance (SPR).³¹ The single and strong SPR bands indicate the formation of Ag nanoparticles through transverse and longitudinal resonances which are spherical in shape.³² The absorbance spectra of silica nanoparticles absorbed at 320 nm represent the specific peak for Si-O-Si bond which confirms the presence of silica nanoparticles. After the deposition of Ag nanoparticles onto the SiO₂ spheres, broad and less intense peak appeared at 432.22 nm (SiO₂ in Ag hydrosol A) and sharp and high intense peak appeared at 430.66 nm (SiO₂ in Ag hydrosol B) due to the increase in the local refractive index of the surrounding medium for the Ag nanospheres caused by the formation of silica nanospheres and Mie Plasmon resonance excitation from the Ag nanoparticles.³³ There is a slight red shift in absorption wavelength with increasing the size of the silver nanoparticles exhibiting stronger Plasmon resonance.³⁴⁻³⁵ The quantitative analysis of silver hydrosol A and B using SEM images Fig. 7 (e-f) shows the size distribution of different silver nanoparticles. The normal curve function which show average size distribution of silver hydrosol A and B. (See Fig. S3[†]). Thus in case of silver hydrosol B the increase in the intensity is due to participation of more no of particles for Surface Plasmon Resonance compare to silver hydrosol A. This elucidates a difference of 2 nm in the UV analysis for Ag@SiO₂ A and B.

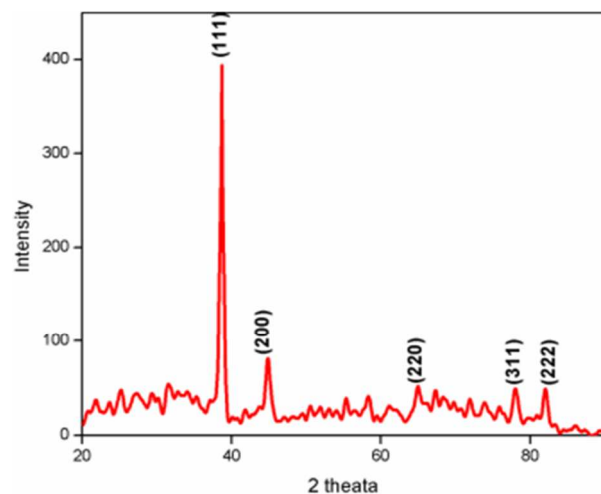


Fig.2. XRD pattern of Ag@SiO₂ nanospheres using hydrosol A

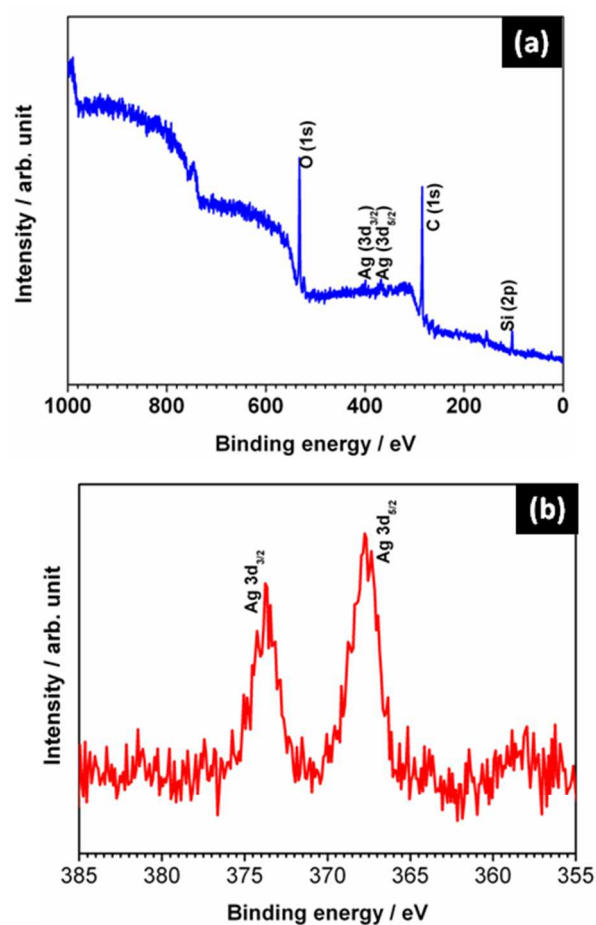


Fig.3. (a) XPS spectra of Ag (hydrosol A) embedded SiO₂ nanospheres (b) corresponding magnified spectra of Ag

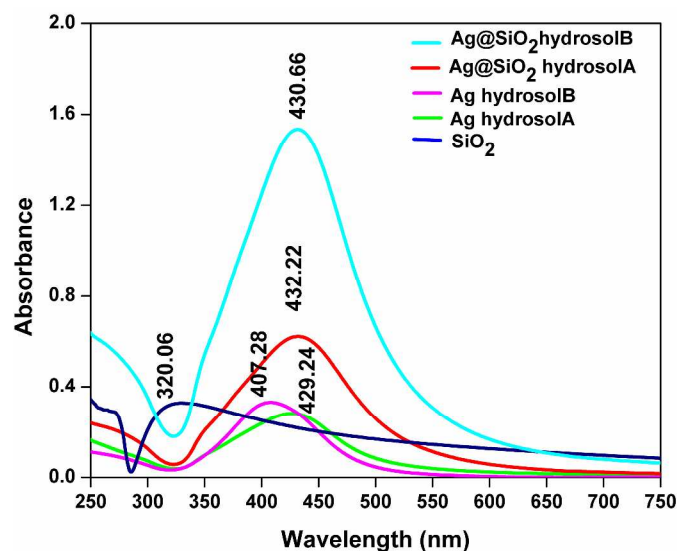
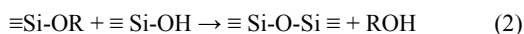
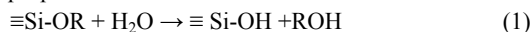


Fig.4. Absorption spectra of Ag hydrosol and Ag@SiO₂ nanospheres

For the growth of silica, two main models have been emerged i.e. the ‘monomer addition model’ and the ‘aggregation growth model’. But still the debate is not over and new growth mechanisms have been postulated.³⁶ Our findings conclude that growth occurs due to aggregation, where the primary particles with broad size distribution are generated in solution over a long time. The growth process of silica nanospheres were sequentially investigated using field emission scanning electron microscopy (see Fig. S2[†])

Growth process of SiO₂ nanospheres is shown in Fig.5. Island like structures with a size of 1-2 μm were formed through a proper combination of constituents (60 ml ethanol, 0.78 ml TEOS, and NH₃, 8pH) which was constantly stirred for 5 mins. An agglomeration of silica beads (150-200 nm) was formed under the same conditions with the addition of 5 ml of distilled water. On increasing the water concentration (10 ml) and pH (10), self-assembled arrays of silica nanospheres (Fig. 6 a-c) were formed. So, the water molecules lead to faster kinetics and promote the nucleation of silica. In addition to this, the presence of ammonia promotes the formation of spherical particles. The effect of solvent and the presence of ammonia are the promising factors for the formation of highly ordered monodispersed spheres.³⁷⁻³⁸

The proposed reaction mechanism is



Here R represents ammonium hydroxide. When a glass slide is dipped into the colloidal solution and then pulled out, the liquid evaporates which pulls the nanospheres together to compact them into a densely-packed monolayer.³⁹ The monodispersity is also confirmed through the cross section image as shown in Fig.6 (d). When the negatively charged glass substrate⁴⁰ reacts with the solution containing positive hydrogen ions, surface diffusion occurs, forming silanol groups. These silanol groups deprotonized the

hydrogen ions and resulted in negatively charged silica nanospheres which is confirmed by zeta potential (see Fig. S6[†]).

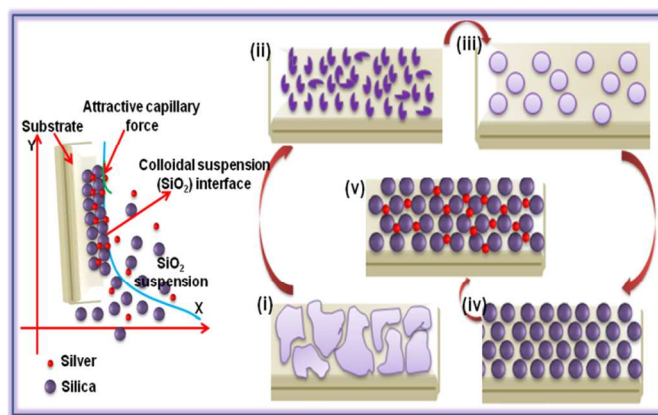


Fig.5. Growth mechanism of silver embedded silica nanospheres (i-absence of H₂O, ii- 5 ml H₂O, iii-10 ml H₂O, iv- 10 ml H₂O +pH10)

In our experiment, the Ag nanoparticles were deposited using two hydrosols as described in the experimental session. Fig. 7(a-b) shows HR-TEM image and its SAED pattern where the hkl value for the plane (111), (222) confirms face centered cubic structure of Ag nanoparticles which well matches with XRD. Also the attachments of AgNPs with SiO₂ nanospheres show a gap of less than 5 nm as shown in Fig. 7(c-d). These give strong evidence of hot spots for SERS studies.

Ag films prepared from both hydrosols show that the Ag nanoparticles are isolated from each other with no aggregation and it is clear that the size of Ag nanoparticles obtained using hydrosol A is bigger than those with Ag hydrosol B. As seen in Fig. 7(e-f) the Ag nanospheres obtained using Ag hydrosol A and B were in the size ranges of 15-20 nm and 5-10 nm respectively. The high degree of super saturation of NaBH₄ leads to the formation of smaller silver nanoparticles. The positively charged silver nanoparticles prepared from hydrosol B cling onto the surface of silica nanospheres due to the negative surface charge of silica (see Fig. S4-S7[†]). As shown in Fig. 8(a-c), the negatively charged silver nanoparticles (hydrosol A) assemble in the nanogap between silica nanoparticles which may be due to the capillary forces⁴¹ and in the present case, the silica nanospheres array can act as the channel. The surface charge of Ag nanoparticles was confirmed by zeta potential analysis (see Fig. S8[†]) and the relationship between interparticle gap and SERS activity for Ag nanoparticle shows a dramatic enhancement when the size is in between 15-20 nm.⁴²⁻⁴⁶ As a result, Ag@SiO₂ nanospheres obtained using Ag hydrosol A are considered as promising SERS substrates owing to their unique morphology. The atomic percentages of Si (35.21at %), O (53.14at %) and Ag (11.65at %) confirm the formation of Ag@SiO₂ nanospheres (Fig. 8h) and color mapping shows the elemental analysis of Ag@SiO₂ (Fig.8(d-g)). The red dots indicate the Ag peaks while the green and blue dots indicate the silicon dioxide.

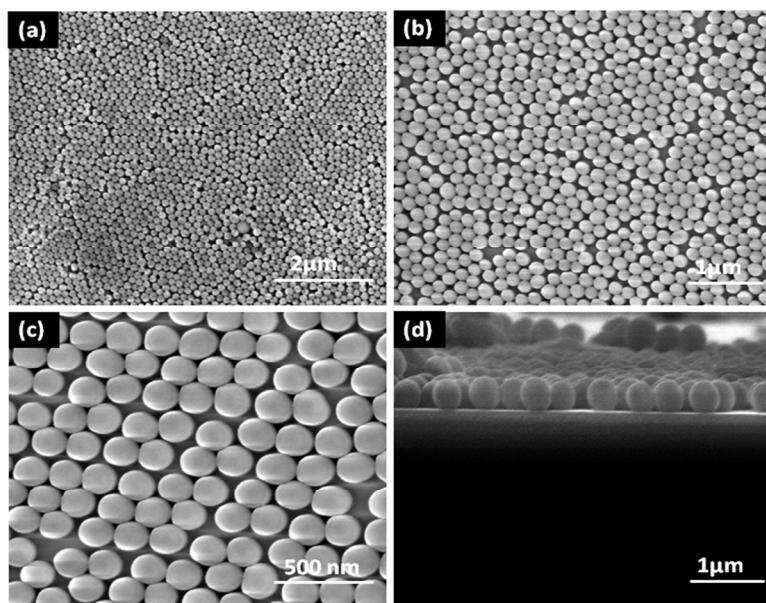


Fig.6. (a-c) FESEM micrographs of SiO₂ with different magnifications (d) cross section image of SiO₂ nanospheres.

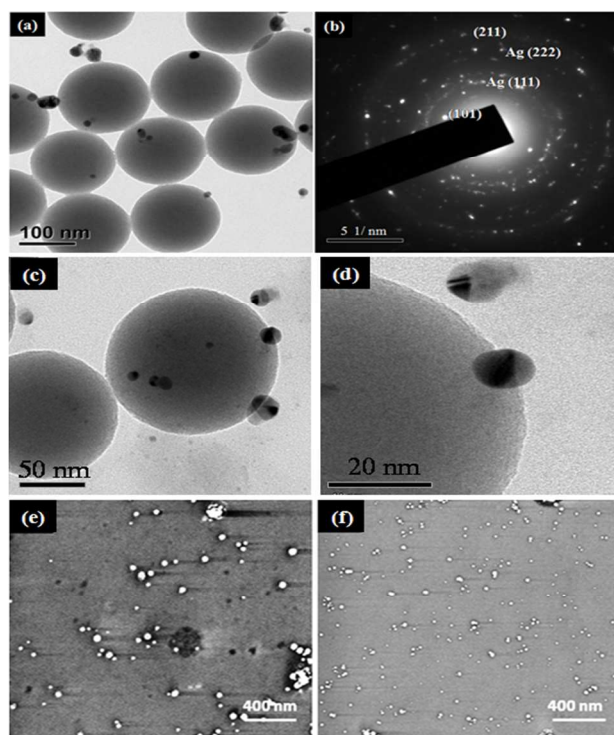


Fig. 7. (a) HR TEM images of Ag@SiO₂ nanospheres for silver hydrosol A (b) SAED pattern (c-d) magnified HRTEM images and FESEM micrographs of Ag nanospheres prepared using (e) hydrosol A (f) hydrosol B

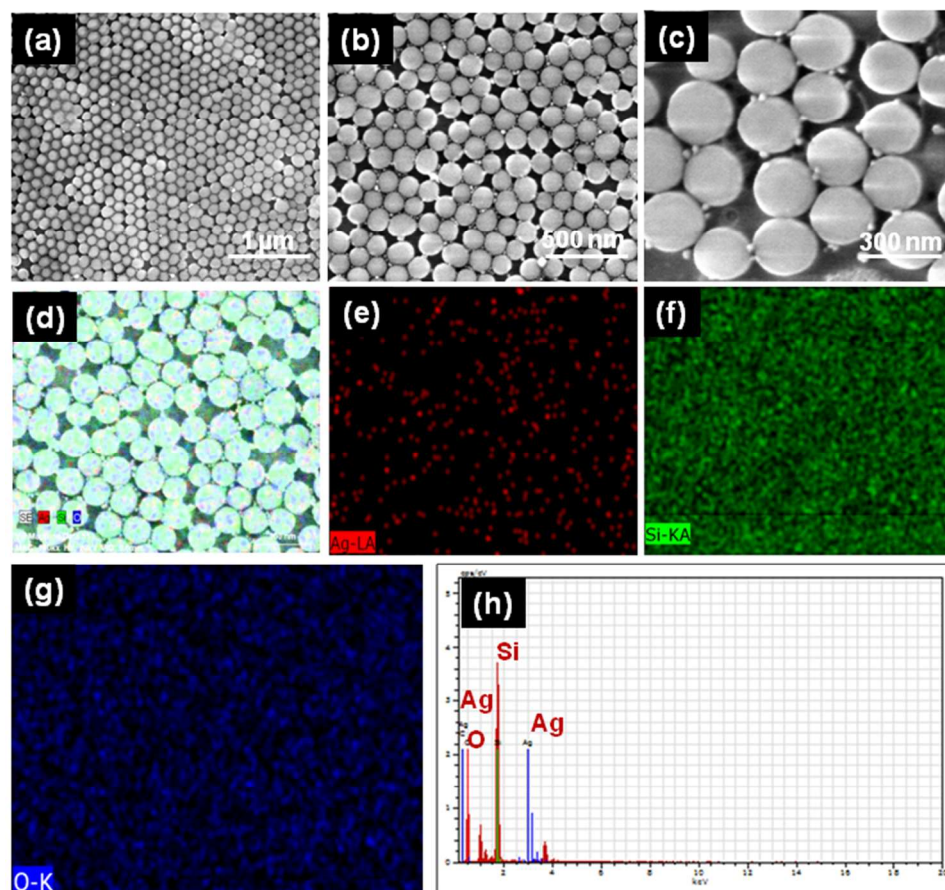


Fig.8. (a-c) FESEM micrographs of Ag@SiO₂ thin films with different magnifications (d-g) color mapping image of Ag@SiO₂ nanospheres (h) EDAX spectra of Ag@SiO₂. [Note: Here Ag represents hydrosol A]

Roughness is one of the most important parameters for SERS. When the molecules are adsorbed to the metallic surfaces and exhibit atomic scale roughness, the Raman signal intensity is enhanced by 10^4 to 10^6 times. Fig. 9(a-b & d-e) represents the 2D and 3D images of SiO₂ and Ag@SiO₂ nanospheres which are identical with the FESEM images. Fig. 9 (c & f) presents the two-dimensional histograms containing surface height values determined from the respective topographies. The obtained SiO₂ and Ag@SiO₂ nanospheres exhibited root-mean-square (RMS) roughness values of 14.9057 and 26.004 nm respectively and show high monodispersity of nanospheres.

The finite-difference time-domain (FDTD) method is adopted using numerical solution-8. Intensity ($|E|^2$) distributions are obtained from 3D FDTD calculations based on the following parameters: SiO₂ (glass) palik material has been used as material,

where the diameter of noble metal nanoparticles was 20 nm and an interparticle gap of 5 and 2.5 nm between silica and silver was chosen. Laser with 514 nm wavelength was employed. The detailed process is illustrated in Fig. 10. The maximum intensity ($|E|^2$) of each noble metal/semiconductor was 112. As the SERS signals were proportional to the value of ($|E|^2$), the 20 nm silver nanoparticles give larger SERS enhancement. Similarly in Fig. 10a, when the gap between silica and silver is around 2.5 nm the hot spots increase and give strong electric field enhancement, while in the case of Fig. 10b, smaller electric field enhancement occurs around the spheres when the nano gap is around 5 nm compared to the gap of 2.5 nm. It means that hotspots are formed between the silica and silver nanospheres and giant SERS enhancement can be obtained.

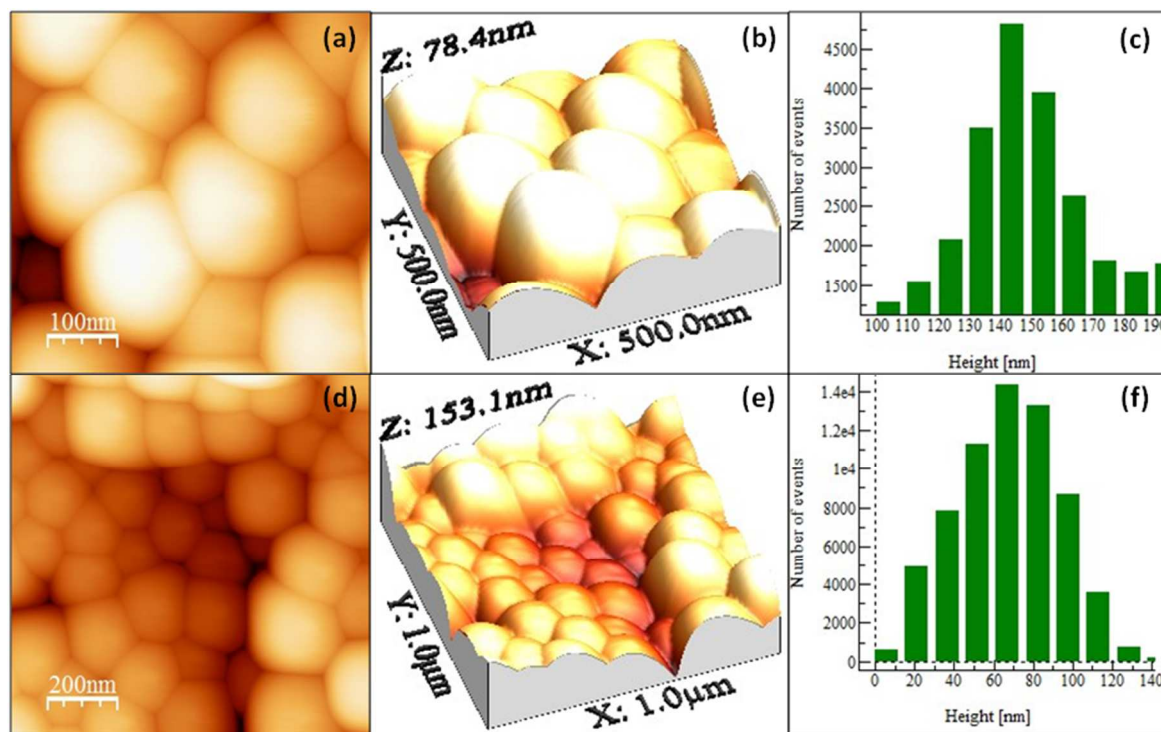


Fig.9. AFM 2D and 3D images of (a-b) SiO₂ nanospheres (d-e) Ag@SiO₂ nanospheres and (c & f) Histograms of SiO₂ and Ag@SiO₂ nanospheres [Note: Here Ag represents hydrosol A]

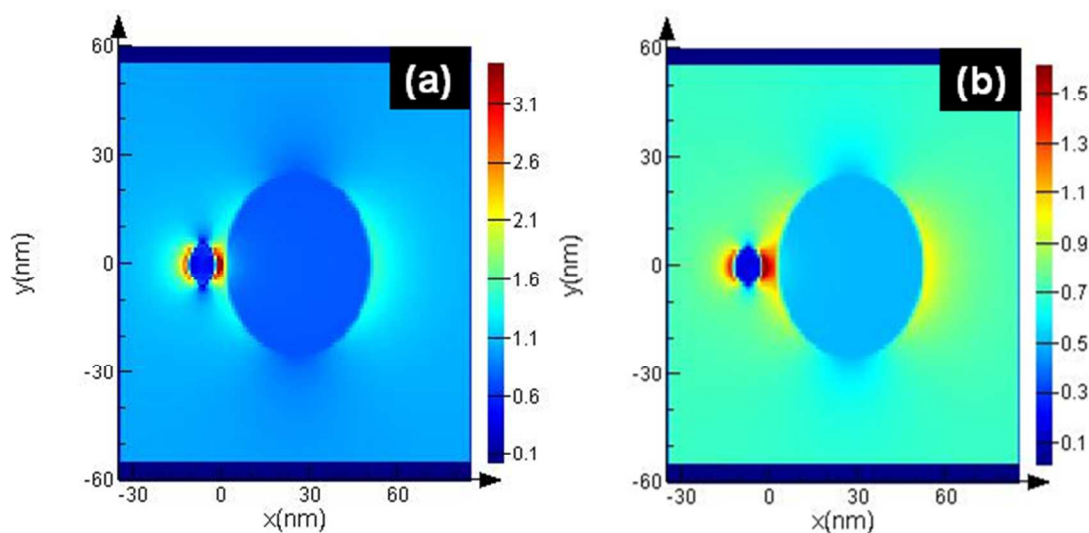


Fig.10. Electric field ($|E|^2$) distributions obtained from 3D FDTD calculations at wavelength 514 nm of (a) 2.5 nm gap (b) 5 nm gap.

3.2. SERS analysis of self-assembled Ag embedded silica thin films

Fig. 11b and 11c show the SERS spectra of R6G with different molar ratios adsorbed on Ag@SiO₂ substrates using Ag hydrosols A and B. Normal Raman Spectrum (NRS) of R6G (Fig. 11a) with a molar concentration of 10⁻⁴ M gets shifted to 612.28, 771, 919, 1194, and 1367 cm⁻¹ while neighbouring peaks at 1527 and 1571.2 cm⁻¹ merge into one broad peak at 1575 cm⁻¹ as shown in Fig. 11c. Also two brother peaks observed at 1355 and 1180 cm⁻¹ shifted to 1367 and 1194 cm⁻¹ respectively on using Ag hydrosol A. The shifting and broadening are due to the binding of chloride ions of R6G with Ag@SiO₂ which provide active sites for Raman enhancement.¹⁰ Nanoscale gaps and sharp points in metal nanostructures are the primary features needed to produce the highest possible enhancement in Raman scattering. Here the interparticle gap between silica and Ag nanoparticles is below 5 nm (Fig. 8c) which results in strong localized plasmon resonance and offers an opportunity to realize notable SERS enhancement in the case of Ag hydrosol A. Electric-field enhancement for Ag nanoparticles assembled on silica contains three types of nanoparticle arrangements, such as isolated nanoparticles, surface-plasma-coupled nanoparticles, and aggregated nanoparticles. Signal enhancement for Ag@SiO₂ using hydrosol A is attributed due to the surface-plasma-coupled nanoparticles arrangement¹⁷, since, the

enhancement increases rapidly when the spacing between neighbouring nanoparticles reduces (see Fig. S4 †).

In the case of Ag@SiO₂ using Ag hydrosol B, no noticeable intensity was observed for 10⁻¹² M and 10⁻⁸ M due to the aggregated arrangement of Ag nanoparticles on monodispersed silica nanospheres. Fig. 11(a) shows normal Raman spectra of R6G for 10⁻⁸ and 10⁻⁴ M and the same on using silver sol A, while Fig. 11(b) and (c) show the SERS spectra of Ag@SiO₂ using Ag hydrosol A and Ag hydrosol B respectively, where the maximum SERS is obtained for hydrosol A only. The use of Rhodamine 6G as a SERS probe using a 532 nm laser has been greatly discouraged, given the actual signal is coming from the so-called SER(R)S.⁴⁷ The Rhodamine 6G is also in resonance with the laser. For confirmation of SERS we have taken the SERS spectra of R6G 10⁻¹¹ molar concentration using 632 nm laser wavelength in Fig. 11(d). A similar work by Kudelski et al.⁴⁸ shows that SERS effect is “switched on” in measurements with the red excitation radiation and the resonance Raman Effect for R6G molecules is “switched off”. However the intensity recorded by them is very low for R6G using Ag@SiO₂. In our case the peaks are shifted to ± 5 cm⁻¹ comparing to 514 nm wavelength and gives a much more high intense peak for R6G 10⁻¹¹ M.

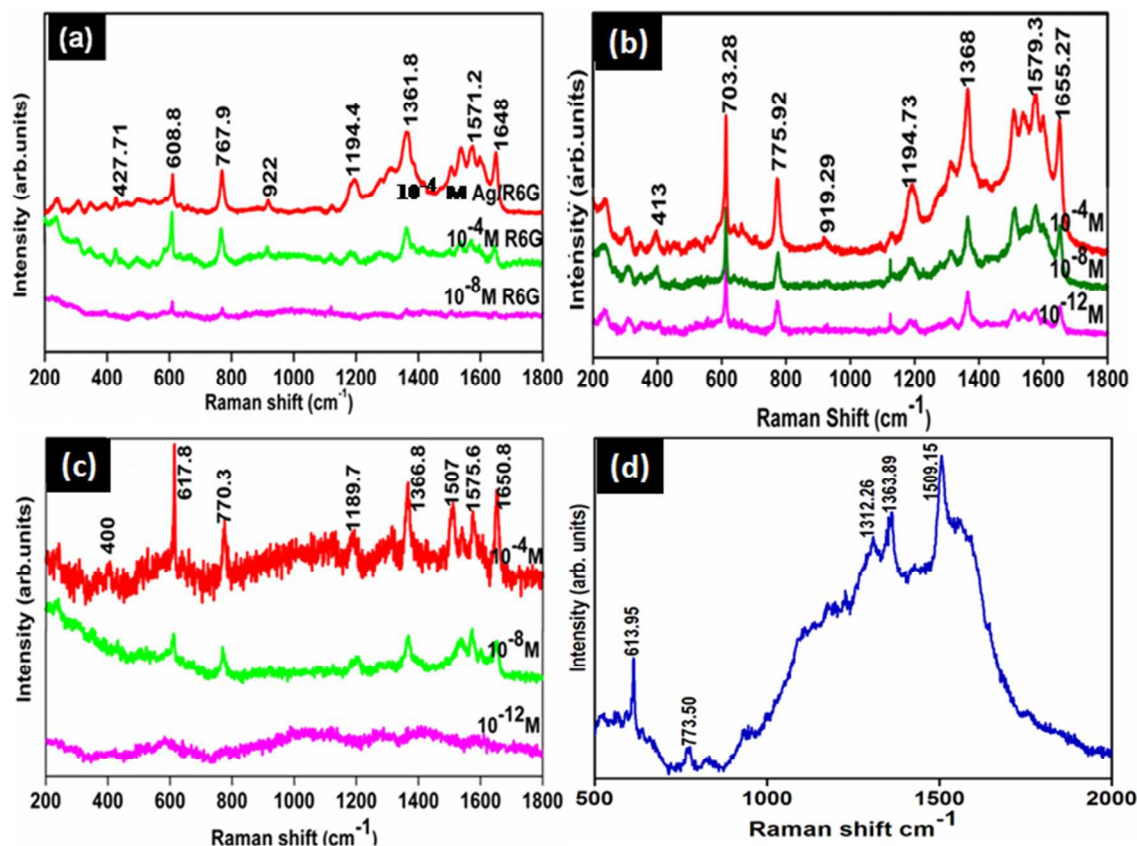


Fig. 11. (a) SERS spectra of Ag/R6G and Normal Raman Spectra of R6G with 10⁻⁴ M and 10⁻⁸ M (b) SERS spectra Ag@SiO₂ nanospheres (Ag hydrosol A) (c) SERS spectra Ag@SiO₂ nanospheres (Ag hydrosol B) (d) R6G 10⁻¹¹ M SERS spectra for Ag@SiO₂ nanospheres (Ag hydrosol A) using 632nm laser wavelength.

ARTICLE

Hence it is concluded that the size of the Ag nanoparticles and the interparticle gap between silica and Ag nanoparticles are the primary factors for SERS enhancement. The Enhancement factor was also calculated according to equation.²⁶

$$EF = \frac{I_{SERS}}{I_{bulk}} \times \frac{N_{bulk}}{N_{surf}}$$

Where I_{surf} and I_{bulk} are the integrated intensities of R6G molecules adsorbed on Ag@SiO₂ SERS substrate for 10⁻¹¹ M and 10⁻³ M of R6G bulk, respectively. N_{surf} and N_{bulk} are the corresponding numbers of R6G molecules adsorbed on the SERS substrate and in the bulk solution effectively illuminated by the laser beam, respectively. $N_{bulk} = AhC_{bulk}NA$, where A is the area of the laser focal spot, h is the focal depth of the laser, and h is 13 μm according to the work.²⁶ C_{bulk} is the concentration of R6G bulk solution, here $C_{bulk} = 10^{-3}$ M, NA is the Avogadro constant

$$N_{surf} = \frac{C_{SERS}VN_A A}{\pi r^2}$$

The above calculations (see Fig.S11†) were done for the 20 μl R6G solution (1 × 10⁻³ M) and the R6G - adsorbed on Ag@SiO₂ (1 × 10⁻¹¹ M, 20 μl) which were spread on the 1 × 1 cm² prepare substrate. A laser spot area of 5 μm and power of (15 mW) was applied with an accumulation number of 1 sec for all recordings. The N_{bulk}/N_{surf} value is calculated to be 32.656 × 10⁵ and I_{SERS}/I_{bulk} are about 7.79 for the vibration peak at 1367 cm⁻¹ (see Fig.S11†). The EF value is calculated to be about 7.79 × 10⁸. Similarly we have also optimized the condition for lowest detection of 10⁻¹⁸ M based on their optical images as shown in the Fig.12. In optical images we can easily able to identify the dye absorbance as shown in Red color. The overall interpretation shows that when laser falls on red colored area we could expect enhanced Raman due to the linker molecule and charge transfer of dye into substrate. In case of 10⁻¹⁸ M the peaks were very weak but the spectra at 1367 cm⁻¹ can be easily absorbed while the remaining peaks were shows very weak intensity. This confirms the contribution of highly monodispersed silica nanospheres for the SERS enhancement.

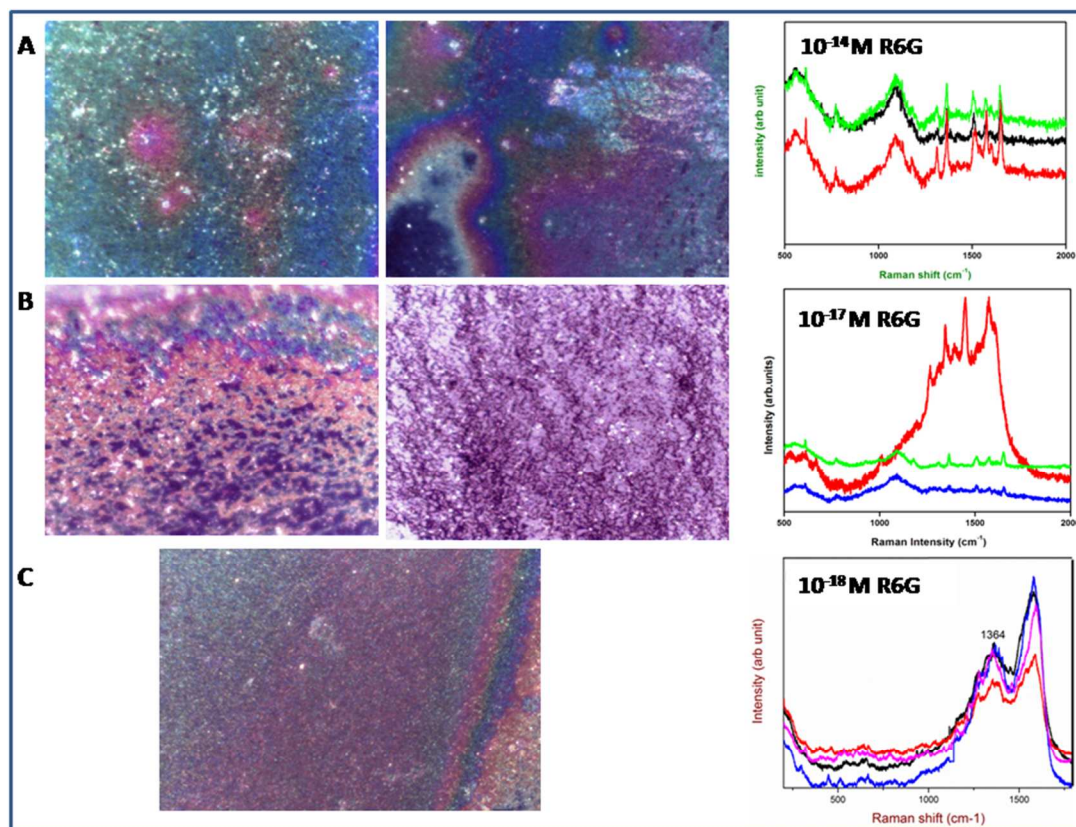


Fig.12. Optical images of Ag@SiO₂ nanospheres film using confocal Raman spectrometer (a) R6G 10⁻¹⁴ M (b) R6G 10⁻¹⁷ M (c) R6G 10⁻¹⁸ M

The designed substrates show good reproducibility that is confirmed through FESEM images (see Fig.S9 †). A previous study on nanowires⁴² shows the tendency to form clusters after drying the analyte solution. But in the present study the nanospheres shows no bundling and clustering. The results show the good stability of nanospheres against the analyte. A substrate of 1 x 1 cm was dispersed with R6G with a molar of 10^{-11} and spectra were recorded for 30 spots to check the reproducibility of film (Fig.13). The substrate shows highly intense and uniform peak over the substrate. The stability of prepared colloid was checked over the different substrates and different period of time which confirms the consistency of solution and film Fig.13 (d-e). Fig.13 (d-e) represents the SERS spectra of R6G over ITO and silicon substrate. This confirms that the present method is different from other techniques where the nanogaps formation is not defined over the substrate. The Fig. 13b clearly shows that the silver prepared using hydrosol A with a size of 15 nm exactly cling in between silica nanospheres due to the low nanogap between two spheres, whereas the bigger particle are not able to adhere inside the obtained gap (See Fig.S1 †). So this confirms that the nanogaps formation in our substrate leads to good

efficiency and reproducibility towards development of ultrasensitive SERS substrate. An Ag@SiO₂ nanosphere for SERS application has been extensively analyzed in the present study, and it has been shown that a simple vertical deposition can be used to generate reproducible SERS substrates. The present method is technically sound and shows perfect morphology and designing procedure for the creation of hot spots. Moreover this method is of very low cost and is reproducible compared to other methods as shown in the comparative study (Table 1).

For the confirmation of SERS we have chosen another probe molecule melamine. Melamine is an organic chemical material and is mainly used to produce melamine-formaldehyde resins for glues, adhesives, and plastics. For boosting of protein content it has been used in dairy products such as milk.⁴⁹ The present substrate shows the detection of Melamine in liquid up to 10^{-8} molar concentration as shown in Fig. 14. Fig. 14 represents the SERS spectra of melamine in liquid for increasing concentration up to 10^{-8} M on to Ag@SiO₂ substrate. The most prominent peak at 682 cm^{-1} is assigned to the ring breathing mode II and involves in-plane deformation of the triazine ring in melamine molecules.²⁴

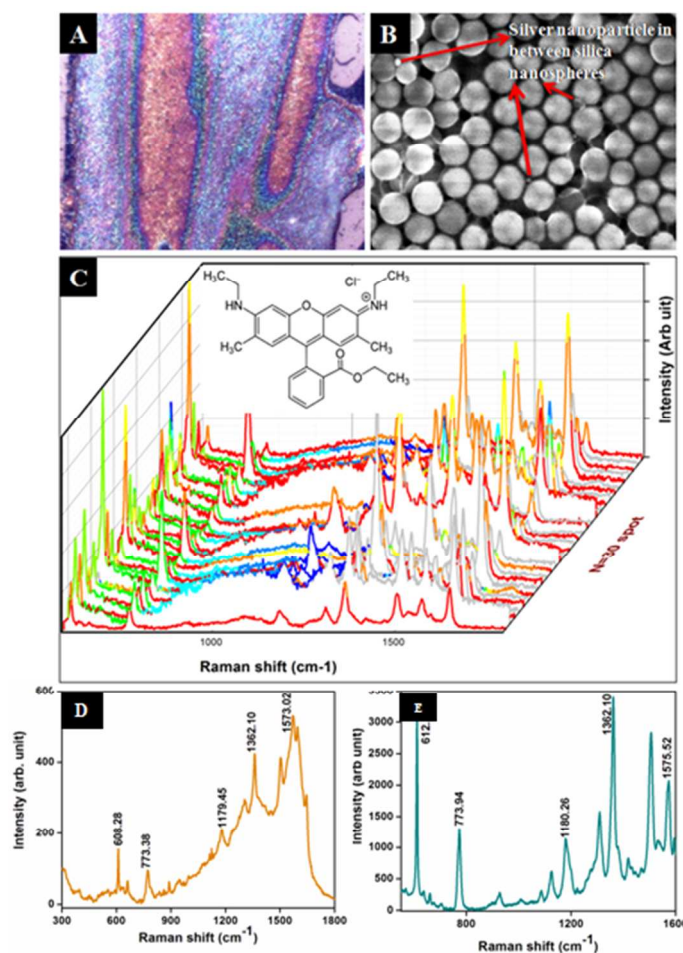


Fig.13. (a) Optical image of Ag@SiO₂ nanospheres film consist of R6G 10^{-11} M (Optical image of 10^{-11} M R6G on Ag@SiO₂ nanospheres film) (b) Corresponding FE-SEM image (Ag@SiO₂ nanospheres using Ag hydrosol A) (c) SERS spectra for 30 spots and chemical structure of R6G (d) SERS spectra of R6G for 10^{-11} M on ITO and (e) silicon substrate.

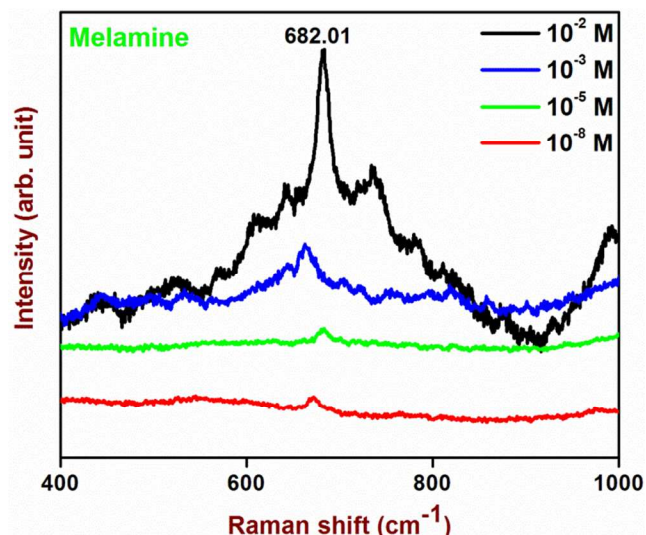


Fig.14. SERS spectra of melamine enhanced by Ag@SiO₂ (Ag hydrosol A) film for different molar concentrations.

4. Conclusion

Despite significant progresses in the field of plasmonic, it seems that SERS-active substrates with unique morphology, uniformity, stability, reproducibility and high enhancement factor are rather difficult to achieve. The technique used in the present study facilitates the fabrication of active SERS substrates consisting of highly monodispersed silica nanospheres array and with an ideal reproducible surface morphology where strong SERS signals can be generated from minimal quantities of adsorbed analyte. This method has the potential for application in SERS micro-detection devices. The ratio of ammonia to water was a key factor for the formation of self assembled nanospheres array. Adsorption behavior of R6G on Ag@SiO₂ nanospheres, particle size of Ag nanospheres and interparticle gap between Ag@SiO₂ nanospheres play important role in the fabrication of highly active surface enhanced Raman scattering substrates. It is also found that the SERS effect from noble metal and metal oxide films has its own limits whereas metal embedded metal oxide films show very high enhancement compared to ordinary ones. The electric field signal enhancement (hotspots) was confirmed through FDTD model. Ag@SiO₂ substrates show good response to probe molecule R6G. Also it has been used as inspecting device for detection of trace chemical like melamine which is harmful to the environment. This simple and ultrasensitive substrate shows us the importance of nanostructures and their nanogaps arrangement within substrate. The substrate could be further used as a Raman reporter for early diagnosis of cancer and biosensor studies.

5. Acknowledgement

The authors want to thank Dr. Joydeep Chowdhury and Sannak Dutta Roy, Chemical physics and materials science research group, Sammilani Mahavidyalaya, University of Kolkata for FDTD simulation.

6. Notes

^aDepartment of Nanoscience and Technology, Bharathiar University, Coimbatore-641 046, India.

Email: dmraj800@yahoo.com

^bEnvironmental & Water Technology, Centre of Innovation, Ngee Ann Polytechnic, Singapore 599489, Singapore

^cNational Institute of Advanced Industrial Science and Technology (AIST), 2266-98 Anagahora, Shimoshidami, Moriyama-ku, Nagoya 463-8560, Japan.

^dCenter for Nanofibers and Nanotechnology, Department of Mechanical Engineering, National University of Singapore, Singapore 117576

7. References

- 1) Juan J. Giner-Casares, Luis M. Liz-Marzán, *Nano Today*, 2014, **9**, 365.
- 2) S. Bhavya, R. F. Renee, I. H. Anne, R. Emilie and R. P. Van Duyne, *Mater. Today*, 2012, **15**, 16.
- 3) M. Fleischmann, P. J. Hendra and A. J. McMullan, *Chem. Phys.* 1974, **26**, 163.
- 4) G. Xiao, B. Ying, Q. Chao and J. Chaoyang, *J. Chem. Comm.* 2012, **48**, 7003.
- 5) J. C. Richard and J. T. Martin, *J. Raman Spectros.* 2008, **39**, 1313.
- 6) Y. Zao, X. Xibin, L. Xibo, L. Jiangshan, W. Weidong, T. Yongjian and Y. Yougen, *Appl. Surf. Sci.* 2011, **258**, 212.
- 7) H. Hwang, S. Kim and Y. S. Man, *Lab on Chip*, 2011, **11**, 87.
- 8) G. Kumari and C. Narayana *J. Phys. Chem. Lett.* 2012, **3**, 1130.
- 9) G. Sun and G. Grundmeier, *Thin Solid Films*, 2006, **515**, 126.
- 10) Y. Kobayashi, H. Katakami, E. Mine, D. Nagao, M. Konno and L.M. L. Marzan, *J. Colloid Interface Sci.* 2005, **283**, 392.
- 11) M. C Wu, M.P. Lin, S.W Chen, P.H Lee, J.H Li and W.F Su, *RSC Adv.* 2014, **4**, 10043
- 12) Y. Yang, Z.Y. Li, K. Yamaguchi, M. Tanemura, Z. Huang, D. Jiang, Y. Chen, F. Zhou and M. Nogami, *Nanoscale*, 2012, **4**, 2663.
- 13) Z. Jiang and C. Liu, *J. Phys. Chem. B* 2003, **107**, 12411.
- 14) Y. Liu, Y. Zhang, H. Ding, S. Xu, M. Li, F. Kong, Y. Luo and G. Li, *J. Mater. Chem. A*, 2013, **1**, 3362.
- 15) V.E. Subramanian, E. Wolf and P.V. Kamat, *J. Phys. Chem. B*, 2001, **105**, 11439.
- 16) X.Q. Wang, T.J. He, H. Wen, C.Y. Xu, J. Zuo and F.C. Liu, *Spectrochim. Acta, Part A*, 1997, **53**, 2495.
- 17) R. Xu, W. Xiao-Dong, W. Liu, X. Xiao-Na, L. Yue-Qiang and A. Ji, *Chin. Phys. B* 2012, **2**, 025202.

- 18) L. Shijia, L. Li, G. Hao, Y. Wu and L. Feng, *Dyes Pigm.* 2012, **95**, 473.
- 19) B. Li-Li, M. M. Shannon, L. Cheng-Du and D. Sheng, *J. Raman Spectrosc.* 2003, **34**, 394.
- 20) F. G. Kirsty and A. P. Girard, *J. Phys. Chem C* 2010, **114**, 22406.
- 21) W. Ming-Chung, L. Min-Ping, C. Shih-Wen, L. Pei-Huan, L. Jia-Han and S. Wei-Fang *RSC Adv*, 2014, **4**, 10043.
- 22) Panarian, A.Y.; Terekhov, S.N.; Kholostov, K.I.; Bondarenko V.P. *Appl. Surf. Sci.* 2010, **256**, 6969.
- 23) Wang, Y. Q. Ma, S.; Yang, Q.Q.; Li, X.J. *Appl. Surf. Sci.* 2012, **258**, 5881.
- 24) Zhang, K.W.X.; Niu, C. and Wang.Y. *ACS Appl. Mater. Interf.* 2014, **6**, 1272.
- 25) Han, Y. Liu, S.; Liu, B.; Jiang, C. and Zhang, Z, *RSC Adv.* 2014, **4**, 2776
- 26) Jing Chen, Gaowu Qin, Wen Shen, Yiyan Li and Biswajit Das, *J. Mater. Chem. C*, 2015, **3**, 1309.
- 27) P. Suresh, J. Sundaramurthy, D. Mangalaraj, D. Nataraj, D. Rajarathnam and M. P. Srinivasan, *J. Colloid Interface Sci*, 2011, **363**, 51.
- 28) Y. W. Lu, X. W. Du, a J. Sun, and X. Han *J. Appl. Phys.* 2006, **100**, 063512.
- 29) L. Kai, J. Xiaotong, T. Aiwei, Z. Xibin, M. Huan and W. Yingfeng, *Integr. Ferroelectr*, 2012, **136**, 9.
- 30) K. Wang, X. Zhang, C. Niu and Y. Wang, *Appl. Mater. Interfac.* 2014, **6**, 1272.
- 31) G. Upender, R. Sathyavathi, B. Raju, C. Bansal and R. Narayana, *J. Mole. Struct*, 2012, **1012**, 56.
- 32) S. Werner, F. Arthur and B. Ernst, *J. Colloid Interface Sci*, 1968, **26**, 62.
- 33) O. Keng-Liang, H. Ting-Chu, L. Yu-Chuan and Y. Kuang-Hsuan. *Mater Chem Phy.* 2012, **135**, 892.
- 34) K. Nogi, M. Naito and Toyokazu Okoyama, *Nanoparticle technology-Handbook*.
- 35) Tzounis, R. C. Caceres, L. Schellkopf, D. Jehnichen, D. Fischer, C. Cai, P. Uhlmann and Manfred Stamm, *RSC Adv.*, 2014, **4**, 17846
- 36) Camille C. M. C. Carcouët, Marcel W. P. Van de Put, Brahim Mezari Pieter C. M. M. Magusin, Jozua Laven, Paul H. H. Bomans, Heiner Friedrich, A. Catarina C. Esteves, Nico A. J. M. Sommerdijk, Rolf A. T. M. van Benthem, and Gijsbertus de. *Nano lett*, 2014, **14**, 1433.
- 37) R. Kota Sreenivasa, K. El-hami, K. Tsutomu, M. Kazumi and M. Keisuke, *J. Colloid Interface Sci*, 2005, **289**, 125.
- 38) G. Schatz, *Acta Phys. Pol. A*, 2009, **115**, 431.
- 39) I. Hyungsoon, C. B. Kyle, C. L. Nathan, L. H. Christy and H. Sang-Hyun. *Nano Lett*, 2010, **10**, 2231
- 40) W. L. W. Hau, D. W. Trau, N. J. Sucher, M. Wong and Y. Zohar, *J. Micromech. Microeng*, 2003, **13**, 272.
- 41) S. H. Im, Y. T. Lim, and D. J. Suh, O. O. Park, *Adv. Mater.*, 2002, **19**, 1367
- 42) J. B. Jackson and N. J. Halas, *J. Phys. Chem. B*, 2001, **105**, 2743.
- 43) Stampelcoskie and K. G. Scaiano, *J. C. J. Phys. Chem. C*, 2011, **115**, 1403.
- 44) Kleinman, S. L., Frontiera, R. R, Henry, A. I.; Dieringer and J. A. Van Duyne, *R. P. Phys. Chem. Chem. Phys.* 2013, **15**, 21.
- 45) Wang, H. H. Liu, C. Y. Wu, S. B. Liu, N. W. Peng and C. Y. Chan, T. H.; Hsu, C. F.; Wang, J. K.; Wang, Y. L. *Adv. Mater.* 2006, **18**, 491
- 46) J. N. Chen, T. Martensson, K. A. Dick, K. Deppert, H. Q. Xu, L. Samuelson and H. X. Xu, *Nanotechnology* 2008, **19**, 275712.
- 47) Martin Moskovits, *Phys. Chem. Chem. Phys.*, 2013, **15**, 5301.
- 48) A. Kudelski and S. Wojtysiak, *J. Phys. Chem. C* 2012, **116**, 16167.
- 49) J. M. Li, W. F. Ma, C. Wei, L. J. You, J. Guo, J. Hu, and C. C. Wang, *Langmuir* 2011, **27**, 14539.

Table 1. Comparative SERS performance on Ag@SiO₂ nanostructures

Substrate	Dye used and Detection limit	Enhancement factor	Experimental method	Optical Quality and Remarks	Arrangement of silver over Silica and nanostructures	Ref
Silica nanoparticles	R6G up to 10 ⁻⁵ M	1.09x 10 ⁶	Spin coating and vacuum deposition	Fair. polycrystal structure with low detection limit.	Silver on monolayer silica. Structure not defined	20
n-type porous silicon nanostructures	R6G up to 10 ⁻¹⁰ M	-----	Colloidal method	Poor. Difficulty in arrangement of pore diameter. Hot spots decrease while porosity increases	Randomly arranged Ag nanoclusters in porous silicon	22
Boron-doped Single crystal silicon(sc-Si) wafers	R6G up to 10 ⁻¹⁵ M	----	Hydrothermal etching method	Fair. Silver agglomeration and interfacial strain. No confirmation of hotspots	Ag/Si nanopillar like structure	23
Silica colloidal microspheres	R6G up to 10 ⁻¹² M	1.68x 10 ⁷	Colloidal method	Poor. Aggregated silver around silica and no proof for hot spots.	Silica colloidal microspheres with silver	24
Silica wafer	R6G up to 10 ⁻¹⁸ M	10 ¹⁶	Modified colloidal	Fair. Uniform spherewith agglomerated silver arrangement and no hot spots.	Ag Nanocontacts onto Silica	25
Ag@SiO ₂ nanospheres Glass substrate	R6G up to 10 ⁻¹⁸ M	7.79x10 ⁸	Vertical deposition (Dip coating)	Excellent. Highly monodispersed spheres with maximum hot spots.	Silver embedded silica nanospheres	Present Work